Supporting Information

Computational structure determination of novel Metal-Organic Frameworks

Mohammad Wahiduzzaman,[a] Sujing Wang,[b] Benjamin J. Sikora,[a] Christian Serre,*[b] and Guillaume Maurin,*[a]

[a]*Institut Charles Gerhardt Montpellier, UMR 5253 CNRS, ENSCM-UM, Université Montpellier, 34095 Montpellier cedex 05, France Email: Guillaume.Maurin@univ-montp2.fr*

[b]*Institut des Matériaux Poreux de Paris, FRE 2000 CNRS, Ecole Normale Supérieure, Ecole Supérieure de Physique et de Chimie Industrielles de Paris, PSL Research University, 75005 Paris Email: christian.serre@ens.fr*

AASBU simulation flow:

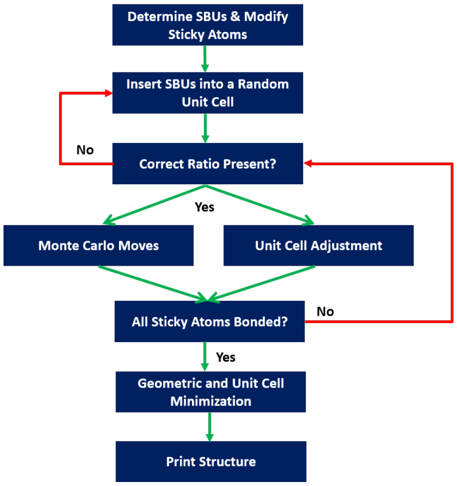

Fig. S1 Work flow of a typical AASBU simulation.

Construction of MOF-5:

Both the Zn_4O SBU and BDC linkers were treated independent units where six carboxylates carbons in the Zn_4O SBU and two carboxylate carbon atoms in the BDC linkers are defined as possible linkage points (sticky-atoms) as depicted in Figure S1-a & -b). A first series of AASBU simulation has been performed with one Zn_4O SBU plus three BDC linkers in the simulation box to match the connectivity of the constituents. A 1:3 ratio of Zn_4O to BDC linkers resembles into a simple cubic cell where the BDC linkers are allowed to take any random orientations along the edges. As a result a pcu net has been generated, however such unrestricted assembly results in much lower symmetries (e.g., P222) than the experimental geometry. One should bear in mind that two carboxylate groups in the opposite sides the

Zn_4O tetrahedron are basically sitting in two planes perpendicular to each other. Therefore, assembly of one Zn_4O to three BDC linkers wouldn't be possible to obtain expected MOF-5 pore topology ensuring that BDC linkers and carboxylates attached to the Zn_4O SBUs are aligned in the same plane. However, by doubling the number SBUs and linkers, i.e., a mixture of two Zn_4O SBUs with six BDC linkers in conjunction with the proper dihedral angle restriction (i.e., a benzene ring of the BDC linker should form 180° dihedral angles with adjacent carboxylates of the Zn4O SBUs), nicely reproduces the experimentally observed high symmetry (*Fm3m*) face center cubic system.[1] Such construction procedure also illustrates the importance of the inclusion of dihedral angle term in our AASBU energy cost function for the assembly of highly symmetric ordered systems.

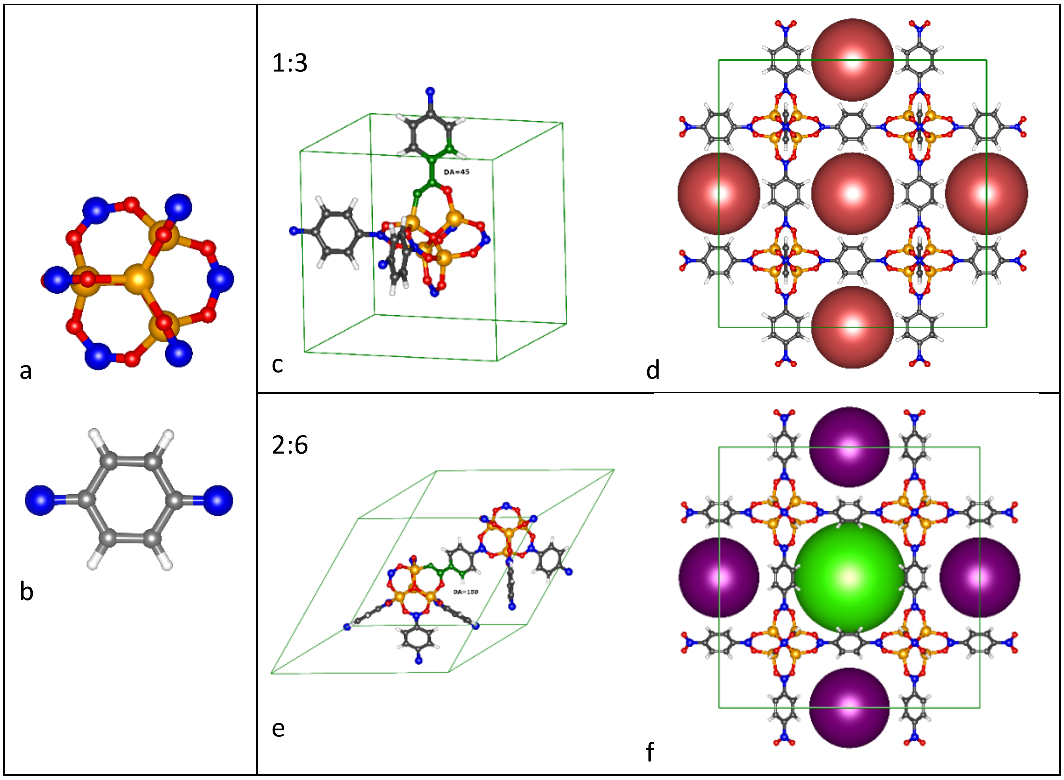

Fig. S2 AASBU construction of MOF-5. A mixture of one Zn_4O cluster (a) with three BDC linkers (b) per asymmetric cell leads to a simple cubic unit cell (c-d). The exclusion of dihedral angle correction in the AASBU energy cost function yields random arrangement of BDC linkers with Zn_4O cluster and hence different pore distribution than experimental structure. The example shown in the upper-right panel (subfig. c-d) is a special case where BDC linkers connect to the carboxylates of the Zn_4O cluster resulting a dihedral angles of 45° (highlighted in green). The bottom-right panel shows the AASBU construction of MOF-5 framework with a mixture of two Zn_4O cluster and six BDC linkers per asymmetric cell. The inclusion of dihedral term in the energy cost function produces a large pore surrounded by six small pores, as observed in experimental geometry.

Construction of UiO-66:

Applying the same approach, UiO-66[2] framework has been reproduced by mixing one Zr_6O_8 cluster to six BDC linkers. The Zr_6 cluster was modeled with 12 sticky-atoms in position of carboxylate carbons while BDC linkers remained the same as of MOF-5. Unlike, MOF-5 SBU, here the polyhedron edges of the Zr_6O_8 are bridged by carboxylates forming three perpendicular planes. Each of this plane consists four carboxylates, make it possible to construct expected pore geometry with one Zr_6O_8 cluster and six BDC linkers per asymmetric unit cell.

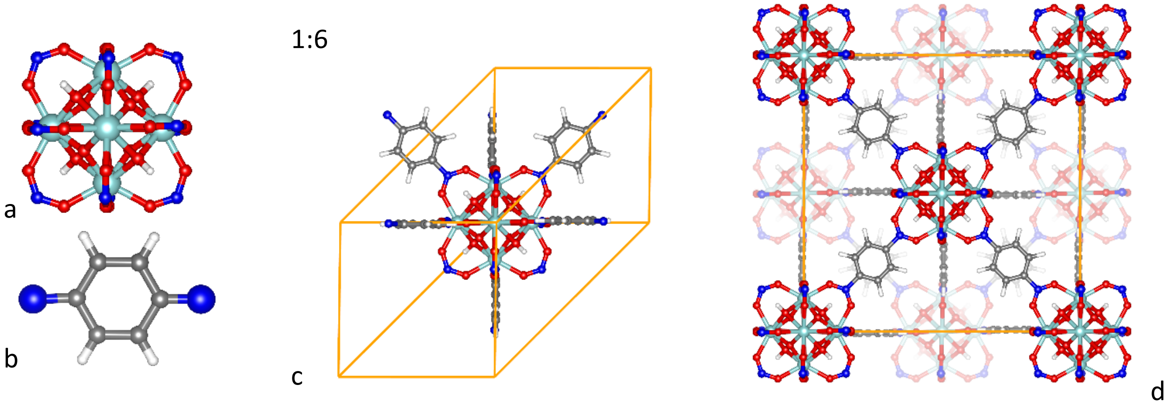

Fig. S3 AASBU construction of UiO-66. A mixture of 1:6 ratio of the Zr_6O_8 cluster (a) to BDC linkers (b) leads to a rhombohedral primitive cell (b) and conventional cubic unit cell (d). Blue spheres represent the predefined connection points (sticky atoms).

Dihedral angles in MIP-202 and MIP-204:

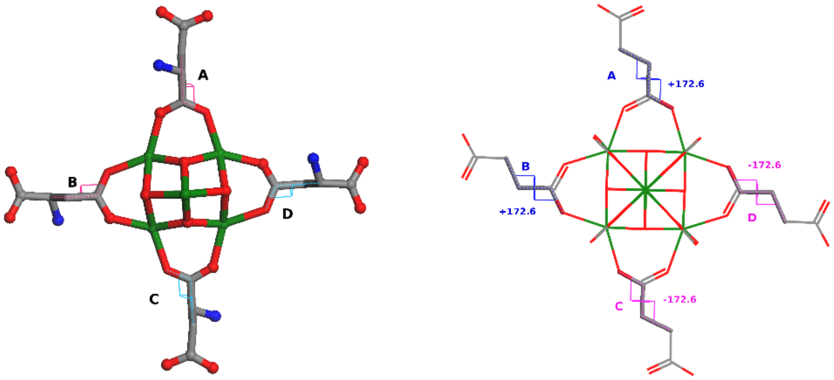

Fig. S4 Dihedral angle definitions of MIP-202 (left panel) where, A=B=C=D = 90°, and MIP-204 (right panel) where A = B = 172.6° and C = D = -172.6°.

AASBU Simulation Details for the successful Generation of Candidate Structures:

Lennard-Jones (LJ) potential parameters:

Table S1 Lennard-Jones (LJ) potential parameters used in the AASBU simulations for constructing the MOFs reported in this study. L^{org} and L^{inorg} are the sticky atoms in the organic and inorganic units, respectively, while CA refers to the central dummy atoms of the building units.

Atom pairs	Interaction type	ϵ_{ij} [kcal mol^{-1}]	σ_{ij} [Å]
L^{org} _ L^{inorg}	LJ attractive	100	0.2
L^{org} _ L^{org}	LJ repulsive	4[a]	3.0
L^{inorg} _ L^{inorg}	LJ repulsive	4[a]	3.0
CA^{org} _ CA^{inorg}	LJ repulsive	4[a]	3.0
CA^{org} _ CA^{org}	LJ repulsive	4[a]	4.0
CA^{inorg} _ CA^{inorg}	LJ repulsive	4[a]	8.0

[a] these ϵ parameters used only to tune the steepness of the repulsive part of the potential, i.e., no attractive contributions are added to the total energy cost function.

Input settings:

As our AASBU implementation is written in C++ programing language, we have employed a large number of functionalities from the C++/boost libraries,[3] including the mersenne_twister_engine model for pseudo_random_number_generator.[4] We have observed that the seed values of this random number generator — which is based on the local time of the machine — greatly influence the elapsed time required for the successful assembly of a candidate structure. As such, the total number of required MC steps might be very different even starting with same input parameters. Therefore, we came to a decision that instead of employing very large MC steps per run, it is advantageous to run AASBU simulation through an external loop with new seed values for each single runs with ~1milion MC steps. For example, in the cases of MOF-5 and UIO-66, where the local geometry (i.e., internal coordinates) of the SBUs and BDC linkers are rather simple and well characterized, a single MC simulation led to the assembly of the expected geometries, while for MIP-202,-203, and -204, multiple external loops were required. And thus, we have adopted our AASBU implementation in such a way that a single AASBU run comprises several internal loops starting with fresh seed values until an expected assembly is successful.

Structural properties of the newly developed MOFs:

Table S2 Structural parameters of novel MOFs determined by AASBU simulations.

	Inorganic and organic units with ratios	Lattice type and symmetry	Lattice Parameters (Å)	Pore Volume cm^3g^{-1}
MIP-202	Zr_6O_8 (M_6…L_{12}) + Aspartate 1:6	FCC P213(198)	a=17.8339	0.10
MIP-203	Zr_6O_8 (M_6…L_8) + Succinate 1:4	Orthorhombic I2MM (44)	a=11.8932 b=10.0351 c=19.8764	0.27
MIP-204	Zr_6O_8 (M_6…L_8) + Succinate 1:4	Tetragonal P-4N2 (118)	a=b=11.0922 c=19.7058	0.24

Pore Size Distribution (PSD):

The geometric methodology reported by Gelb and Gubbins [5] was used to calculate the pore size distributions (PSD) of the DFT-optimized MIP-202, -203,and -204 structures., as depicted in Fig. S6. In these calculations, the van der Waals parameters of the framework atoms were adopted from Universal Force Field (UFF).[6]

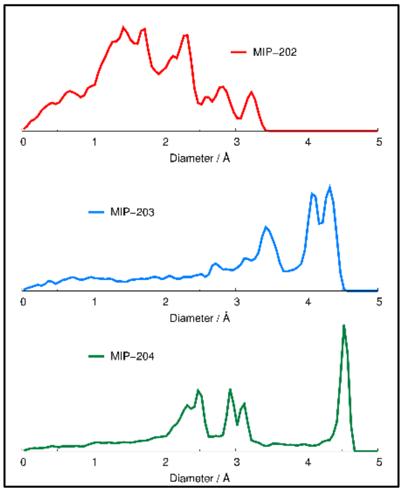

Fig. S5 Pore size distribution of MIP-202,-203,-204 frameworks.

DFT calculations:

The geometry optimization calculations were performed at the density functional level of theory (DFT) using the Quickstep module [7] of the CP2K program [8,9] employing the Gaussian Plane Wave (GPW) formalism. The general gradient approximation (GGA) to the exchange-correlation functional according to Perdew-Burke-Ernzerhof (PBE)[10] was used in combination of Grimme's DFT-D3 semi-empirical dispersion corrections.[11,12] Triple-ζ plus valence polarized Gaussian-type basis sets (TZVP-MOLOPT) were considered for all atoms, except for the Zr metal centers, where double-ζ plus valence polarization functions (DZVP-MOLOPT) were employed.[13] The interactions between core electrons and valence shells of the atoms were described by the pseudopotentials derived by Goedecker, Teter, and Hutter (GTH).[14–16] The auxiliary plane wave basis sets were truncated at 400 Ry.

Pore volume calculations:

The free pore volume (V_{pore}) of the MOFs were further calculated using a geometric method[17] with the consideration of a probe molecule of 0 Å.[17] The Lennard-Jones size parameters of the framework atoms were also taken from UFF.[6]

Typical synthesis of MIP-202:

L-aspartic acid (1.4 g) was transferred into a 25 mL round bottom flask, 5 mL of water was added to disperse the linker. $ZrCl_4$ (1.15 g) was added by portion into the water suspension, leading to a clear colorless solution. Another 5 mL of water was added to flush the inner face of the flask, trying to wash as much as possible the $ZrCl_4$ powder down into the solution. The reaction was kept at reflux for 12-24 hours (110 °C). After cooling down to room temperature, the expected product of MIP-202(Zr) was collected by filtration, washed with water/EtOH at room temperature and air dry. This preparation method could be applied to either smaller scale syntheses or larger scale ones when a reflux apparatus with suitable size is involved.

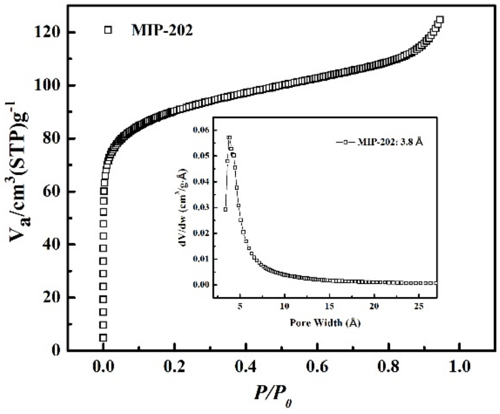

Fig. S6 Nitrogen adsorption isotherm of MIP-202 obtained at 77 K.

Typical Synthesis of MIP-203:

$ZrCl_4$ (230 mg, 1 mmol) and succinic acid (480 mg, 4 mmol) were added into a Teflon reactor (23 mL) followed by adding formic acid (4 mL). The resulting mixture was stirred at room temperature for 20 minutes and was sealed in an autoclave. The reaction was heated at 120 °C for 72 hours. After cooling down to room temperature, the crude product was filtered, washed with EtOH and dried in air.

Typical Synthesis of MIP-204:

$ZrCl_4$ (460 mg, 2 mmol) and succinic acid (480 mg, 4 mmol) were added into a Teflon reactor (23 mL) followed by adding formic acid (4 mL). The resulting mixture was stirred at room temperature for 20 minutes and was sealed in an autoclave. The reaction was heated at 120 °C for 72 hours. After cooling down to room temperature, the crude product was filtered, washed with EtOH and dried in air.

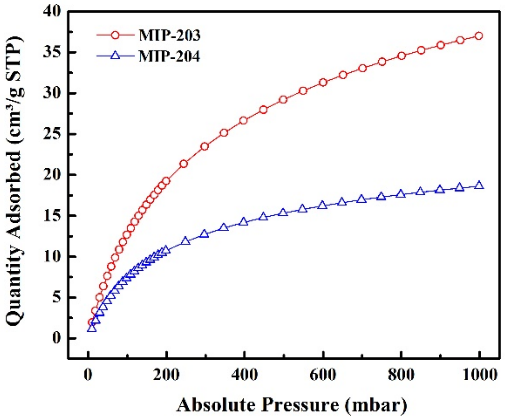

Fig. S7 Carbon dioxide adsorption isotherms of MIP-203 and MIP-204 obtained at 273 K.

References

1 M. Eddaoudi, J. Kim, N. Rosi, D. Vodak, J. Wachter, M. O'Keeffe and O. M. Yaghi, *Science*, 2002, **295**, 469–72.

2 J. H. Cavka, S. Jakobsen, U. Olsbye, N. Guillou, C. Lamberti, S. Bordiga and K. P. Lillerud, *J. Am. Chem. Soc.*, 2008, **130**, 13850–13851.

3 boost, http://www.boost.org.

4 M. Matsumoto and T. Nishimura, *ACM Trans. Model. Comput. Simul.*, 1998, **8**, 3–30.

5 L. D. Gelb and K. E. Gubbins, *Langmuir*, 1999, **15**, 305–308.

6 a. K. Rappe, C. J. Casewit, K. S. Colwell, W. a. Goddard and W. M. Skiff, *J. Am. Chem. Soc.*, 1992, **114**, 10024–10035.

7 J. VandeVondele, M. Krack, F. Mohamed, M. Parrinello, T. Chassaing and J. Hutter, *Comput. Phys. Commun.*, 2005, **167**, 103–128.

8 J. Hutter, M. Iannuzzi, F. Schiffmann and J. VandeVondele, *Wiley Interdiscip. Rev. Comput. Mol. Sci.*, 2014, **4**, 15–25.

9 The CP2K developers group, http://www.cp2k.org.

10 J. P. Perdew, K. Burke and M. Ernzerhof, *Phys. Rev. Lett.*, 1996, **77**, 3865–3868.

11 S. Grimme, J. Antony, S. Ehrlich and H. Krieg, *J. Chem. Phys.*, 2010, **132**, 154104.

12 S. Grimme, *J. Comput. Chem.*, 2004, **25**, 1463–73.

13 J. VandeVondele and J. Hutter, *J. Chem. Phys.*, 2007, **127**, 114105.

14 S. Goedecker, M. Teter and J. Hutter, *Phys. Rev. B*, 1996, **54**, 1703–1710.

15 M. Krack, *Theor. Chem. Acc.*, 2005, **114**, 145–152.

16 C. Hartwigsen, S. Goedecker and J. Hutter, *Phys. Rev. B*, 1998, **58**, 3641–3662.

17 T. Duren, F. Millange, G. Ferey, K. S. Walton and R. Q. Snurr, *J. Phys. Chem. C*, 2007, **111**, 15350–15356.